To be published in Int. J. Solids Structures in 2022

Plastic Buckling of Columns at the Micron Scale

Kim L. Nielsen[a] and John W. Hutchinson[b1]
[a]Mechanical Engineering Department, Technical University of Denmark
[b]School of Engineering and Applied Sciences, Harvard University

Abstract: Clamped-clamped compressed wide metal columns with length to thickness ratios such that they undergo plastic buckling are considered. Further, the thickness of the columns is assumed to be in the range of microns to tens of microns, typical of elements comprising some of the small-scale lattice materials currently being produced. The strengthening effects associated with plastic strain gradients are expected to influence buckling behavior, and the columns are analyzed using several versions of the available strain gradient plasticity theories. The primary focus is the onset of plastic buckling as predicted by bifurcation from the state of uniform compression. However, a numerical post-buckling study is carried out for one class of strain gradient theories for columns with initial imperfections to ascertain if the buckling predictions stemming from this class of theory are realistic.

1. Introduction

Recent advances in metal processing techniques such as 3D printing have made it possible to manufacture small-scale metal structures and lattice materials with column and plate elements whose thicknesses are in the micron range. This paper explores the increase in plastic buckling resistance expected due to the phenomenon of plastic strain gradient hardening when micron-scale beams and plates are compressed into the plastic range. This paper is contributed to a special issue of the *International Journal of Solids and Structures* to celebrate the 70th birthday of one of the major contributors to the plastic buckling of structures, Stelios Kyriakides. The two-volume research monograph, Kyriakides and Corona (2007) and Kyriakides and Lee (2020), deals with large structures, primarily off-shore structures with chapters covering aspects pf plastic buckling in all its richness. While the present paper makes contact with plastic buckling in the large-scale range, the primary emphasis is on the increase in plastic buckling strength that is expected to occur for columns and plates whose thicknesses are in the range from microns to tens of microns. Buckling, whether it be in columns, plates, or shells, usually involves an abrupt change from a relatively uniform compressive state to deformations involving significant

[1] Telephone and e-mail of corresponding author: 617-495-2848, hutchinson@husm.harvard.edu

bending. If buckling occurs in the plastic range and if the thickness of the structural element is on the order of microns, one can expect that plastic strain gradients driven by the bending will give rise to an increase in buckling resistance. It is this increase in buckling resistance which is investigated in this paper for compressed wide columns, that is, plates bending in only one direction. The wide columns will be taken to be clamped at both ends and compressed uniformly prior to buckling. Buckling associated with bifurcation from the perfectly straight configuration will be analyzed by employing both an exact 2D plane strain formulation and a simpler 1D 'beam' analysis based on Euler-Bernoulli kinematics. Several of the available versions of strain gradient plasticity will be used to expose the sensitivity of the strengthening prediction to the details of the constitutive theory.

The mechanics of column buckling under compression in the plastic range took decades to unfold. Engesser's (1889) tangent modulus load was superseded by von Karman's (1910) reduced modulus load governing stability. Years passed until the importance of the reduced modulus load was overturned by Shanley's (1947) observation that the lowest load for the onset of plastic buckling occurs under increasing load such that the tangent modulus load is indeed the primary critical load of interest for buckling. Shortly thereafter, Hill (1958) placed plastic buckling on a firm mathematical footing within a general continuum mechanics framework, accounting for the fact that bifurcation in the plastic range can occur as a loss of uniqueness without a loss of stability of the uniform state. Additional issues were discovered and addressed in the 1950's and 60's related to the constraint the shape of the yield surface has on plastic buckling predictions for plates and shells. These considerations are not of primary concern to wide column buckling because both the pre-buckling and post-buckling stress states are dominantly plane strain compression.

2. Elevation of the incremental bending stiffness due to the plastic strain gradient

The key to understanding the increase in plastic buckling resistance of a column or plate in the micron range is the increase in incremental bending stiffness predicted by strain gradient plasticity. We begin by presenting the incremental bending stiffness for a wide column, or plate, that has been compressed uniformly into the plastic range and then subject to increments of additional uniform compressive strain and uniform curvature, all under conditions of plane strain. The increments of compression and curvature are constrained such that continued plastic

straining occurs across the entire cross-section of the column, consistent with Shanley's condition discussed later in the paper. With the geometry and coordinates defined as specified in Fig. 1, the current strain component parallel to the column is $\varepsilon_{11} = -\varepsilon_0$ and the imposed increment of strain is $\dot{\varepsilon}_{11} = -\dot{\varepsilon}_0 - \dot{\kappa} x_2$ with $\varepsilon_0 > 0$ in compression and κ as the curvature of the centerline. The condition of continuing compressive plastic strain across the entire thickness requires places a constraint on $\dot{\varepsilon}_0$ and $\dot{\kappa}$ which will be presented below. With P as the horizontal compressive force/depth (depth is out-of-the-plane) and M as the moment/depth about the 3-direction, the incremental relations from the uniform compressive state for the constitutive models being considered are $\dot{P} = S\dot{\varepsilon}_0$ and $\dot{M} = D\dot{\kappa}$ with S and D as the incremental stretching and bending stiffnesses per unit depth.

Throughout this paper, plane strain conditions are assumed such that the out-of-plane strains vanish, i.e., $\varepsilon_{13} = \varepsilon_{23} = \varepsilon_{33} = 0$. In addition, except for the FEM simulations in Section 6, attention will be restricted to materials that are elastically and plastically incompressible. Let E be the elastic Young's modulus, σ_Y the initial yield stress in uniaxial tension (with $-\sigma_Y$ as the yield stress in uniaxial compression). The plane strain elastic modulus for the incompressible material is $E_{ps} = 4E/3$, and the stress component σ_{11} at initial yield in plane strain compression is $\sigma_{11} = -2\sigma_Y/\sqrt{3} \equiv \sigma_{11}^Y$ for all the material models considered here. Denote the incremental 'tangent' modulus for plane strain tension/compression increments by E_t such that $\dot{\sigma}_{11} = E_t \dot{\varepsilon}_{11}$. For all the constitutive models considered in this paper, the incremental plane strain stretching stiffness per unit depth from the state of uniform compression is unaffected by strain gradient effects; it is given by

$$S = 2E_t h \tag{2.1}$$

For all but the non-incremental strain gradient theory introduced later, the incremental bending stiffness per depth following uniform compression for the theories considered here can be written as (the derivation is given in Section 5.1)

$$D = \frac{2}{3} E_t h^3 \left\{ 1 + 3\left(\frac{E_{ps}}{E_t} - 1 \right) \alpha^2 \left(1 - \alpha \tanh\left(1/\alpha\right) \right) \right\} \tag{2.2}$$

Strain gradient effects enter through α which for the three incremental SGP theories considered here has the form

$$\alpha = \sqrt{\left(1 - \frac{E_t}{E_{ps}}\right)\frac{a_2}{3}}\ \frac{\ell}{h} \tag{2.3}$$

where a_2 depends on the specific SGP model and is a dimensionless function of the effective plastic strain, ε_P, in the uniform state prior to application of the bending increment. The length scaling the gradients in the SGP models is ℓ. In the absence of a gradient effect with $\ell \to 0$, the incremental bending stiffness per depth reduces to the prediction of conventional plasticity, $D = 2E_t h^3 / 3$, which, in the absence of plasticity, reduces to the elastic bending stiffness/depth, $D_{elastic} = 2E_{ps} h^3 / 3$.

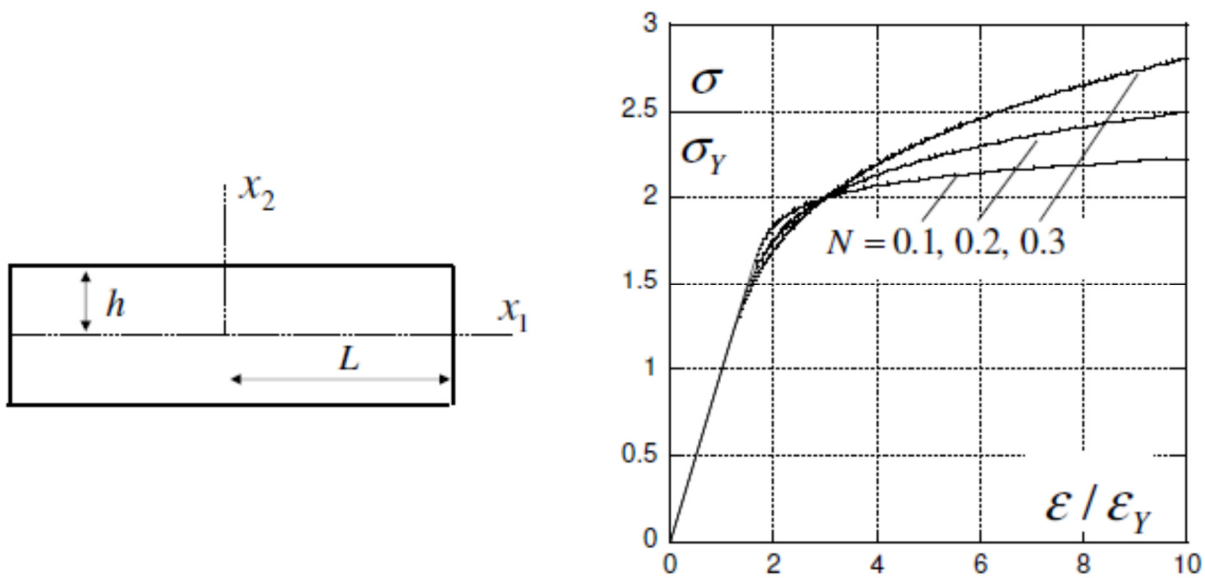

Fig. 1 Cross-sectional geometry for the 2D analysis and uniaxial tension stress-strain curves.

For all the numerical results presented in this paper, the following true stress-log strain curve in uniaxial tension will be used

$$\left.\begin{aligned} &\varepsilon = \sigma / E \ \&\ \varepsilon_P = 0, && \sigma \le \sigma_Y \\ &\varepsilon = \sigma / E + \left((\sigma - \sigma_Y)/k\right)^{1/N}, && \sigma > \sigma_Y \end{aligned}\right\} \tag{2.4}$$

such that beyond yield

$$\sigma = \sigma_0(\varepsilon_P) = \sigma_Y\left(1 + k\varepsilon_P{}^N\right),\ \ \varepsilon_P > 0 \tag{2.5}$$

Here, $\varepsilon_P = \sqrt{2\varepsilon_{ij}^P \varepsilon_{ij}^P / 3}$ is the plastic strain invariant such that the total strain in the uniaxial tensile direction is $\varepsilon = \sigma / E + \varepsilon_P$, N is the strain hardening exponent, and k is a dimensionless coefficient. In uniaxial compression, (2.4) applies with σ and ε changing sign. The curve is plotted in Fig. 1, revealing the smooth transition to plastic flow at the yield stress. The SGP constitutive models will be detailed in Section 4, but here, illustrating how gradient hardening affects bending stiffness, we list the input, a_2, from the three incremental models:

$$\left.\begin{aligned} a_2 &= C_A && \text{Model A} \\ a_2 &= \frac{3\sigma_0(\varepsilon_P)}{E\varepsilon_P} = \frac{3\sigma_Y}{E}\left(\varepsilon_P{}^{-1} + k\varepsilon_P{}^{N-1}\right) && \text{Model B} \\ a_2 &= \frac{3(\sigma_0(\varepsilon_P) - \sigma_Y)}{E\varepsilon_P} = \frac{3\sigma_Y}{E}\left(k\varepsilon_P{}^{N-1}\right) && \text{Model C} \end{aligned}\right\} \tag{2.6}$$

Model A, which assumes a quadratic contribution of the strain gradients to the energy density, was first proposed by Mulhaus and Aifantis (1991). Model B is in the general form suggested by Fleck et al. (2014, 2015), and Model C is a modification of Model B introduced in this paper. Arguments in favor of and antagonistic to these three versions will be presented in Section 4, where their details will be introduced.

The incremental plane strain bending stiffness normalized by the elastic bending stiffness, $D / D_{elastic}$, is plotted in Fig. 2 as a function of the compressive strain for each of the three SGP models in (2.6) for conventional plasticity, $\ell / h = 0$, and for three nonzero values of ℓ / h. The compressive strain ($\varepsilon_{11} = -\varepsilon_0$) is normalized by the compressive strain at initial yield in plane strain, $\varepsilon_{11}^Y = -\sqrt{3}\varepsilon_Y / 2$. While the qualitative trends of the three models displaying the role of strain gradient hardening in elevating the incremental bending stiffness are similar, the quantitative differences are significant. The differences cannot simply be resolved by calibration of the respective models to the strain gradient behavior of a specific material, i.e., by choosing a different value of ℓ for each model for a given material. At this point, the main conclusion to be drawn is that strain gradient hardening has the potential to substantially increase incremental bending stiffness when ℓ / h is not small. Thus, this effect may significantly increase plastic buckling resistance, but there is sensitivity of the predictions to the choice of the SGP model.

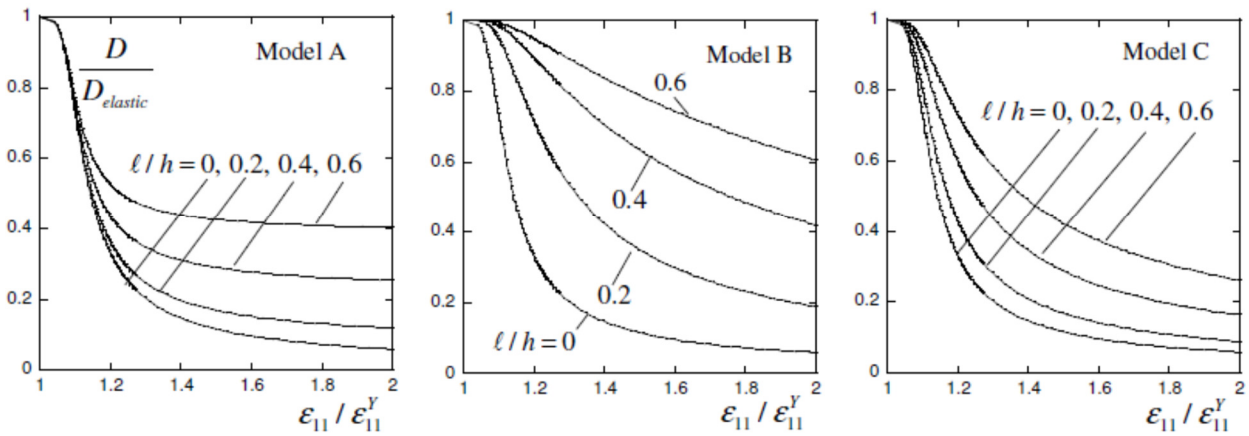

Fig. 2 Incremental bending stiffness normalized by elastic bending stiffness, $D / D_{elastic}$, versus compressive uniform strain normalized by compressive strain at initial yield, $\varepsilon_{11} / \varepsilon_{11}^{Y}$, for the three incremental SGP constitutive models identified in the text for three values of normalized material length scale, ℓ / h, plus the conventional plasticity theory limit, $\ell / h = 0$. In these plots, $\varepsilon_{11}^{Y} = -\sqrt{3}\sigma_Y / 2E$, $\sigma_Y / E = 0.003$, $N = 0.2$ and $k = 1$. For Model A, $C_A = 2$.

Non-incremental SGP theories unrealistically predict that the incremental bending stiffness is the elastic bending stiffness following uniform compression into the plastic range, as shown by Fleck et al. (2014). A discussion of the buckling behavior predicted by the non-incremental SGP models will be presented in Sections 4 and 6.

3. The 1D beam analysis of plastic buckling employing the incremental bending stiffness

The results of the one-dimensional (1D) buckling analysis governed by Euler-Bernoulli beam theory will be easily assessable to anyone familiar with buckling. The classical 1D buckling analysis of a uniform wide column (or, infinitely wide plate) of thickness $2h$ and length $2L$, clamped at its two ends, and compressed in the lengthwise x_1-direction, is governed by the eigenvalue problem

$$D\frac{d^4W}{d^4x_1} + P\frac{d^2W}{d^2x_1} = 0 \text{ with } W = \frac{dW}{dx_1} = 0 \text{ on } x_1 = -L \text{ \& } L \tag{3.1}$$

where $P = -2h\sigma_{11}$ is the compressive force/depth, $W(x_1)$ is the deflection of the beam centerline in the x_2-direction, and D is the bending stiffness/depth. The buckling stress and deflection eigenmode at the onset of buckling are

$$\sigma_{11}^{C} = -\frac{\pi^2}{2}\frac{D}{L^2 h}, \quad W = \frac{W(0)}{2}\left(\cos\left(\frac{\pi x_1}{L}\right)+1\right) \tag{3.2}$$

with $W(0)$ as the eigenmodal amplitude. As already remarked, in the plastic range the incremental bending stiffness/depth, D, must be computed in the sense of Shanley (1947) as the stiffness associated with continuing plastic loading throughout the column. For the column in Section 2 compressed in plane strain the elastic bending stiffness/depth is $D_{elastic} = 2E_{ps}h^3/3$ and the incremental bending stiffness/depth in the plastic range is given by (2.2). The minimum length to thickness ratio for elastic buckling of this column in plane strain compression is $L/h = \pi\sqrt{E/(3\sigma_{11}^{Y})}$ corresponding to $\sigma_{11}^{C} = -\sigma_{11}^{Y}$.

Curves of the critical stress and strain at buckling computed using (3.2) are plotted in Figs. 3 and 4 for conventional plasticity, $\ell/h = 0$, and for three non-zero values of the material gradient parameter, $\ell/h = 0.2, 0.4, 0.6$. (The simplest way to create these plots is to express L/h in terms of ε_P and then evaluate and plot L/h, $\sigma_{11}^{C}/\sigma_{11}^{Y}$ and $\varepsilon_{11}^{C}/\varepsilon_{11}^{Y}$ for values of ε_P). A substantial enhancement of the buckling resistance is predicted for each of the SGP models, but the differences in the predictions between the models are even more notable than that seen for the bending stiffness itself. The results of the exact 2D bifurcation analysis in Section 5 will attest to the accuracy of the simple 1D results in the range of L/h plotted in Figs. 3 and 4.

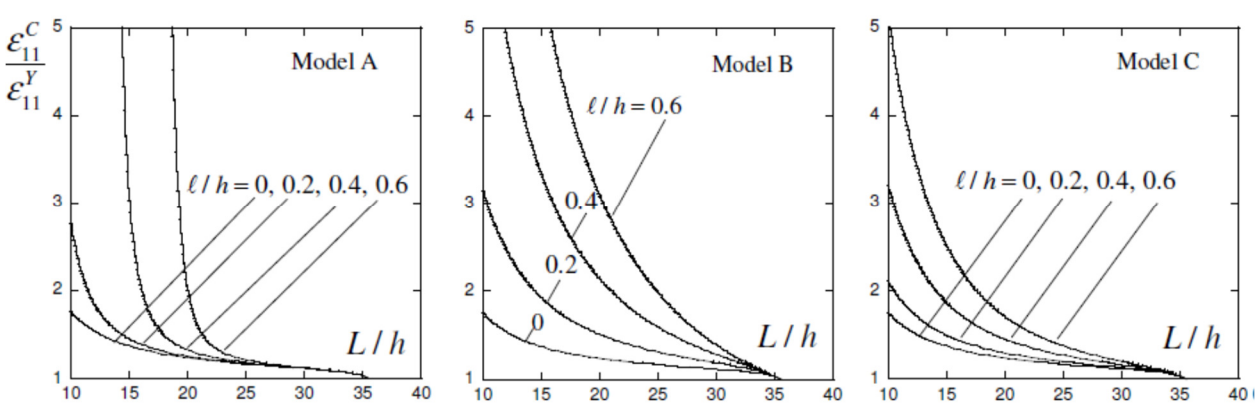

Fig. 3 The results of the 1D plastic buckling analysis of a wide column of thickness $2h$ and length $2L$, which is clamped at both ends and subject to plane strain compression for the three models identified in the text. The incremental bending stiffness/depth D entering (3.2) is presented in (2.2) and Fig. 2. The compressive strain at the onset of buckling ε_{11}^{C} is normalized by the compressive strain at initial yield in plane strain, ε_{11}^{Y}, and plotted for three values of the gradient length parameter ℓ / h. The curve for $\ell / h = 0$ coincides with the limit predicted by Shanley's tangent modulus load of classical plasticity. In these plots, $\varepsilon_{11}^{Y} = -\sqrt{3}\sigma_Y / 2E$, $\sigma_{11}^{Y} = -2\sigma_Y / \sqrt{3}$, $\sigma_Y / E = 0.003$, $N = 0.2$ and $k = 1$. For Model A, $C_A = 2$. Elastic buckling occurs for $L / h > 35.6$.

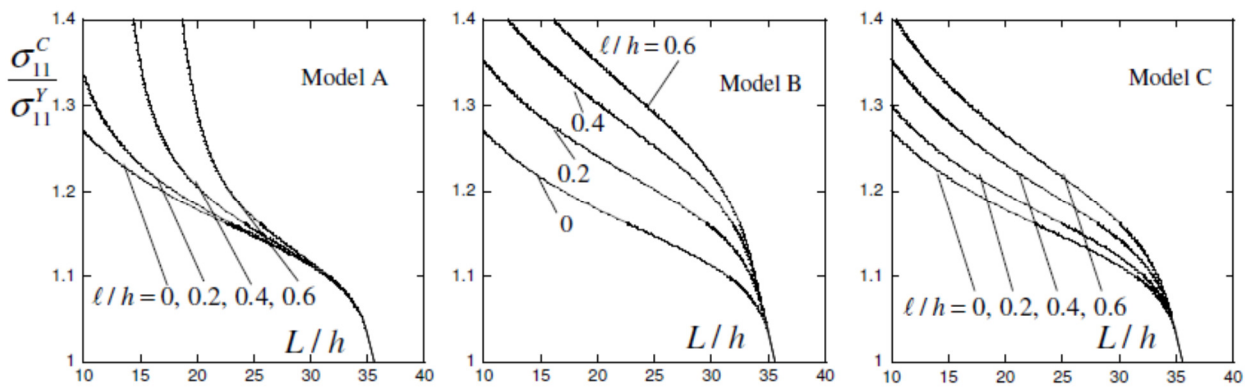

Fig. 4 The normalized stress, $\sigma_{11}^{C} / \sigma_{11}^{Y}$, at buckling as predicted by the 1D theory for the examples considered in Fig. 3.

For plastic buckling, the bifurcation mode at the onset of buckling is the sum of a uniform compression increment determined by the end-shortening increment, $\dot{\Delta} = L\dot{\varepsilon}_0$, and the eigenmode contribution with amplitude $W(0)$ in (3.2). For the 1D model, plastic loading throughout the column requires $\dot{\varepsilon}_0 \geq |\dot{\kappa}| h(1 - \alpha \tanh(1/\alpha))$ (see Section 5.2) along the entire length of the column, which, in turn, requires $\dot{\varepsilon}_0 \geq |W(0)| \pi^2 h(1 - \alpha \tanh(1/\alpha)) / (2L^2)$, or

$$\dot{\Delta} \geq (\pi^2 / 2)(h / L)(1 - \alpha \tanh(1/\alpha)) |W(0)| \text{ and } \dot{P} \geq \frac{\pi^2 Sh}{2L^2}(1 - \alpha \tanh(1/\alpha)) |W(0)| \quad (3.3)$$

At the point where uniqueness of the state of uniform compression is lost, bifurcation takes place under increasing compressive load (Shanley, 1947; Hill, 1958; Sewel, 1963). Post-bifurcation considerations require that elastic loading begins at some point along the column at the onset buckling (Hutchinson,1974), and thus the equality holds in each expression in (3.3).

4. The strain gradient constitutive models

The SGP models will be presented in a curtailed form with minimal background because the details exist in the extensive literature on SGP. Two types of models will be considered, designated incremental and non-incremental. The models considered here in the bifurcation studies are rate-independent and can be regarded as isotropic hardening models. The finite element studies of slightly imperfect columns based on the non-incremental SGP include a small level of visco-plasticity. All the models reduce to their conventional J_2 plasticity counterparts when the material parameter ℓ is set to zero. The elasticity in the models is isotropic; it is incompressible in the bifurcation studies and compressible with a Poisson's ratio, $\nu = 0.3$, in the finite element studies. The notation common to all the models is introduced first. The reader is referred to the papers by Fleck et al. (2014, 2015) for more complete details on the formulation of the models, including the distinctions between incremental and non-incremental theories, and the notation.

A small strain formulation is first introduced and later generalize to large strains. As already introduced, the uniaxial tension stress-strain curve following initial yield at σ_Y is denoted by $\sigma_0(\varepsilon_P)$ for $\varepsilon_P \geq 0$ with $\sigma_0(0) = \sigma_Y$, where $\sigma_0(\varepsilon_P)$ increases monotonically with increasing ε_P. For the uniaxial curve, denote the hardening due to plastic strain by $\Delta\sigma_0(\varepsilon_P) = \sigma_0(\varepsilon_P) - \sigma_Y$. Let $\dot{\varepsilon}_{ij}^P$ be the plastic strain increment, and $\varepsilon_{ij}^P = \int \dot{\varepsilon}_{ij}^P$ as the plastic strain. The total strain is ε_{ij} and the elastic strain is $\varepsilon_{ij}^e = \varepsilon_{ij} - \varepsilon_{ij}^P$. It is essential to distinguish between two effective plastic strain measures. The recoverable effective plastic strain is designated as $\varepsilon_p = \sqrt{2\varepsilon_{ij}^P \varepsilon_{ij}^P / 3}$ which can increase or decrease. The accumulated effective plastic strain used in classical J_2 flow theory is denoted by $e_p = \int \dot{e}_p$, where $\dot{e}_p = \sqrt{2\dot{\varepsilon}_{ij}^P \dot{\varepsilon}_{ij}^P / 3}$; this measure can never decrease and will be referred to as the unrecoverable effective plastic strain.

Under monotonic proportional straining, ε_P and e_p coincide but they generally differ under non-monotonic and/or non-proportional straining. The two corresponding measures of the plastic strain gradients are $\varepsilon_P^* = \sqrt{2\varepsilon_{ij,k}^P \varepsilon_{ij,k}^P / 3}$ and $e_P^* = \int \dot{e}_P^*$ with $\dot{e}_P^* = \sqrt{2\dot{\varepsilon}_{ij,k}^P \dot{\varepsilon}_{ij,k}^P / 3}$, with the first called recoverable and the latter unrecoverable.

Two generalized effective plastic strain quantities are also used which bring in the material length parameter, ℓ. The recoverable measure is $\in_P = \sqrt{\varepsilon_P{}^2 + \ell^2 \varepsilon_P^{*2}}$ and the accumulated, or unrecoverable measure, is $E_P = \int \dot{E}_P$ with $\dot{E}_P = \sqrt{\dot{e}_P{}^2 + \ell^2 \dot{e}_P^{*2}}$. The two sets of measures coincide when the straining is monotonic and proportional i.e., $(\dot{\varepsilon}_{ij}^P, \dot{\varepsilon}_{ij,k}^P) = \dot{\lambda}(\varepsilon_{ij}^0, \varepsilon_{ij,k}^0)$ with $(\varepsilon_{ij}^0, \varepsilon_{ij,k}^0)$ independent of λ, and λ increasing monotonically from zero.

The SGP constitutive relations considered in this paper satisfy the fundamental thermodynamic restrictions on non-negative plastic dissipation proposed by Gudmundson (2004); Gurtin and Anand (2005). The three incremental models are constructed such that the strain gradient contributions are incorporated as part of the recoverable free energy. For the non-incremental constitutive relation considered here, the plastic strain gradients are dissipative and not part of the free energy. The principle of virtual work for all the formulations is

$$\int_V \left\{ \sigma_{ij} \delta\varepsilon_{ij}^e + q_{ij} \delta\varepsilon_{ij}^P + \tau_{ijk} \delta\varepsilon_{ij,k}^P \right\} dV = \int_S \left(T_i \delta u_i + t_{ij} \delta\varepsilon_{ij}^P \right) dS \tag{4.1}$$

with volume of the solid, V, surface, S, displacements, u_i, total strains $\varepsilon_{ij} = (u_{i,j} + u_{j,i})/2$, plastic strains ε_{ij}^P ($\varepsilon_{kk}^P = 0$), and elastic strains $\varepsilon_{ij}^e = \varepsilon_{ij} - \varepsilon_{ij}^P$. The symmetric Cauchy stress is σ_{ij} and the stress quantities work conjugate to increments of ε_{ij}^P and $\varepsilon_{ij,k}^P$ are q_{ij} ($q_{ij} = q_{ji}$, $q_{kk} = 0$) and τ_{ijk} ($\tau_{ijk} = \tau_{jik}$, $\tau_{jjk} = 0$), respectively. The surface tractions are $T_i = \sigma_{ij} n_j$ and $t_{ij} = \tau_{ijk} n_k$ with n_i as the outward unit normal to S. The equilibrium equations are

$$\sigma_{ij,j} = 0, \quad -s_{ij} + q_{ij} - \tau_{ijk,k} = 0 \tag{4.2}$$

with $s_{ij} = \sigma_{ij} - \sigma_{kk}\delta_{ij}/3$. The effective Cauchy stress is $\sigma_e = \sqrt{3 s_{ij} s_{ij} / 2}$. With this background and notation in hand, the incremental SGP models will be introduced first.

4.1 Three incremental SGP models

For the three incremental models considered here, plastic loading requires that the stress, σ_{ij}, is on the current yield surface defined by $\sigma_e = \sigma_0(e_P)$ and that the plastic strain increment is

normal to this yield surface, i.e., $\dot{\varepsilon}_{ij}^{P} = \dot{e}_P m_{ij}$ with $\dot{e}_P \geq 0$ where $m_{ij} = 3s_{ij} / 2\sigma_e$, just as in J_2 flow theory. Note that $\dot{\varepsilon}_P$ is *only* equal to $\dot{e}_P$ under monotonic proportional straining or when $\dot{e}_P = 0$. In general, $\dot{\varepsilon}_P = (2m_{ij}\varepsilon_{ij}^{P} / 3\varepsilon_P)\dot{e}_P$. The gradients of the plastic strain increments are $\dot{\varepsilon}_{ij,k}^{P} = \dot{e}_{P,k} m_{ij} + \dot{e}_P m_{ij,k}$. Define two work-like quantities of the recoverable plastic strain

$$U(\varepsilon_p) = \int_0^{\varepsilon_P} \sigma_0(\varepsilon_p) d\varepsilon_p \text{ and } \Delta U(\varepsilon_p) = \int_0^{\varepsilon_p} \Delta\sigma_0(\varepsilon_p) d\varepsilon_p = U(\varepsilon_p) - \sigma_Y \varepsilon_p \tag{4.3}$$

such that for the stress-strain curve (2.4) used to generate results in this paper,

$$U(\varepsilon_p) = \sigma_Y \left(\varepsilon_p + \frac{k}{N+1} \varepsilon_p^{\,N+1} \right) \text{ and } \Delta U(\varepsilon_p) = \sigma_Y \frac{k}{N+1} \varepsilon_p^{\,N+1} \tag{4.4}$$

Let $\psi_e = \frac{1}{2} L_{ijkl}^{e} \varepsilon_{ij}^{e} \varepsilon_{kl}^{e}$ be the elastic energy density and $\psi_P(\varepsilon_P, \varepsilon_P^*)$ be the recoverable contribution of the plastic strains and plastic strain gradients to the recoverable energy density of the material, $\psi = \psi_e + \psi_p$. The recoverable plastic energy density contributions for three incremental models are

$$\left.\begin{array}{ll} \psi_P = \frac{1}{2} C_A E(\ell \varepsilon_P^*)^2 & \text{Model A} \\ \psi_P = U_P(\in_P) - U_P(\varepsilon_P) & \text{Model B} \\ \psi_P = \Delta U_P(\in_P) - \Delta U_P(\varepsilon_P) & \text{Model C} \end{array}\right\} \tag{4.5}$$

For each model, the recoverable plastic contribution vanishes if the plastic strain gradients are zero and is always non-negative. In Model A, the contribution from the plastic strain gradients is decoupled from the plastic strains, while in Models A and B coupling occurs through the generalized effective plastic strain $\in_P$. The recoverable stress quantities are given by

$$\sigma_{ij} = \frac{\partial \psi_e}{\partial \varepsilon_{ij}^{e}} = L_{ijkl} \varepsilon_{kl}^{e}, \; q_{ij}^{R} = \frac{\partial \psi_P}{\partial \varepsilon_{ij}^{P}}, \; \tau_{ijk}^{R} = \frac{\partial \psi_P}{\partial \varepsilon_{ij,k}^{P}} \tag{4.6}$$

For each of the three incremental SGP models under consideration, the plastic strain gradients make no contribution to the unrecoverable, or dissipated, energy. To date, to our knowledge, no thermodynamically acceptable incremental SGP theory has been proposed with plastic strain gradient contributions to the dissipative energy. The non-negative plastic dissipation increment in the three incremental models considered here is $\dot{d} = \sigma_{ij}\dot{\varepsilon}_{ij}^{P} = \sigma_0(e_P)\dot{e}_p$, and the accumulated plastic dissipation is $d = \int_0^{e_P} \sigma_0(e_p) de_P$. Thus, for these three models, the

unrecoverable contributions to the stress quantities are $q_{ij}^{UR} = s_{ij}$ and $\tau_{ijk}^{UR} = 0$ such that $q_{ij} = s_{ij} + q_{ij}^{R}$ and $\tau_{ijk} = \tau_{ijk}^{R}$. In an increment of deformation, the increment of work of the stresses equals the increments of recoverable and unrecoverable energy densities,

$$\sigma_{ij}\dot{\varepsilon}_{ij}^{e} + q_{ij}\dot{\varepsilon}_{ij}^{P} + \tau_{ijk}\dot{\varepsilon}_{ij,k}^{P} = \dot{\psi} + \dot{d}\,, \tag{4.7}$$

In all three models, $\sigma_{ij} = L_{ijkl}^{e}\varepsilon_{kl}^{e} = L_{ijkl}^{e}(\varepsilon_{kl} - \varepsilon_{kl}^{P})$. In addition:

$$\left.\begin{aligned} q_{ij} &= s_{ij} \\ \tau_{ijk} &= \frac{2}{3}C_A\, E\ell^2\varepsilon_{ij,k}^{P} \end{aligned}\right\} \text{Model A} \tag{4.8}$$

$$\left.\begin{aligned} q_{ij} &= s_{ij} + \frac{2}{3}\left(\frac{\sigma_0(\in_P)}{\in_P} - \frac{\sigma_0(\varepsilon_P)}{\varepsilon_P}\right)\varepsilon_{ij}^{P} \\ \tau_{ijk} &= \frac{2}{3}\ell^2\sigma_0(\in_P)\frac{\varepsilon_{ij,k}^{P}}{\in_P} \end{aligned}\right\} \text{Model B} \tag{4.9}$$

$$\left.\begin{aligned} q_{ij} &= s_{ij} + \frac{2}{3}\left(\frac{\Delta\sigma_0(\in_P)}{\in_P} - \frac{\Delta\sigma_0(\varepsilon_P)}{\varepsilon_P}\right)\varepsilon_{ij}^{P} \\ \tau_{ijk} &= \frac{2}{3}\ell^2\Delta\sigma_0(\in_P)\frac{\varepsilon_{ij,k}^{P}}{\in_P} \end{aligned}\right\} \text{Model C} \tag{4.10}$$

All three of the incremental models are phenomenological but with varying degrees of physics underpinning their construction. Model A is almost certainly the simplest strain gradient plasticity law. It is mathematically attractive because of the quadratic contribution of the plastic strain gradient contributions to the recoverable energy and because this contribution is uncoupled from the contributions of plastic strains. The strain and strain gradient contributions are coupled and on a more equal footing in Models B and C than in Model A in the sense that they make comparable contributions to the hardening and energy when they are of comparable magnitude. The fact that Model A has an additional constitutive parameter, C_A, is indicative of independence of the strain gradient contribution in this model. Model B has the drawback, noted in Fleck et al. (2015), that it can lead to an 'elastic gap' at the onset of plastic yielding in certain instances, such as the case of a layer subject to plane strain tension or compression that has been passivated on its surfaces to block dislocations entering or leaving the surfaces. It is doubtful that

such a gap is realistic, although the relevant experiments do not appear to have been performed to verify or refute the prediction. As can be seen in Figs. 3 and 4, Model B predicts significantly more buckling resistance due to strain gradients than the other two models. Model C is a modification of Model B that eliminates all elastic gaps. The strain gradients in Model C elevate the hardening, $\Delta\sigma_0$, but not the entire yield strength σ_0 as in Model B. Of the three incremental versions considered, we believe Model C has the most favorable attributes. Incremental SGP theories for single crystal plasticity been formulated and analyzed with due consideration to these same issues by Nellemann et al. (2017 a,b).

At the heart of the bifurcation analysis and the implementation of the incremental elastic-plastic boundary value problems is the quadratic expression for the work of the stress increments through their conjugate strain increments, $\varphi = (\dot{\sigma}_{ij}\dot{\varepsilon}^e_{ij} + \dot{q}_{ij}\dot{\varepsilon}^P_{ij} + \dot{\tau}_{ijk}\dot{\varepsilon}^P_{ij,k})/2$ (see, for example, Fleck et al., 2014):

$$2\varphi(\dot{\varepsilon}_{ij}, \dot{e}_P) = L^e_{ijkl}(\dot{\varepsilon}_{ij} - \dot{e}_P m_{ij})(\dot{\varepsilon}_{kl} - \dot{e}_P m_{kl}) + \frac{d\sigma_0(e_p)}{de_p}\dot{e}_p{}^2 + C_A E(\ell\dot{e}^*_P)^2 \quad \text{Model A} \tag{4.11}$$

$$\begin{aligned} 2\varphi(\dot{\varepsilon}_{ij}, \dot{e}_P) = {} & L^e_{ijkl}(\dot{\varepsilon}_{ij} - \dot{e}_P m_{ij})(\dot{\varepsilon}_{kl} - \dot{e}_P m_{kl}) + S(\in_P)\dot{\in}_P{}^2 - S(\varepsilon_P)\dot{\varepsilon}_P{}^2 \\ & + \frac{\sigma_0(\in_P)}{\in_P}\dot{E}_p{}^2 - \frac{\sigma_0(\varepsilon_P)}{\varepsilon_P}\dot{e}_p{}^2 + \frac{d\sigma_0(e_p)}{de_p}\dot{e}_p{}^2 \end{aligned} \quad \text{Model B} \tag{4.12}$$

$$\begin{aligned} 2\varphi(\dot{\varepsilon}_{ij}, \dot{e}_P) = {} & L^e_{ijkl}(\dot{\varepsilon}_{ij} - \dot{e}_P m_{ij})(\dot{\varepsilon}_{kl} - \dot{e}_P m_{kl}) + \Delta S(\in_P)\dot{\in}_P{}^2 - \Delta S(\varepsilon_P)\dot{\varepsilon}_P{}^2 \\ & + \frac{\Delta\sigma_0(\in_P)}{\in_P}\dot{E}_p{}^2 - \frac{\Delta\sigma_0(\varepsilon_P)}{\varepsilon_P}\dot{e}_p{}^2 + \frac{d\sigma_0(e_p)}{de_p}\dot{e}_p{}^2 \end{aligned} \quad \text{Model C} \tag{4.13}$$

where $S(\varepsilon) = d\sigma_0(\varepsilon)/d\varepsilon - \sigma_0(\varepsilon)/\varepsilon$ for Model B and $\Delta S(\varepsilon) = d\Delta\sigma_0(\varepsilon)/d\varepsilon - \Delta\sigma_0(\varepsilon)/\varepsilon$ for Model C. They can be expressed in terms of quantities in the current state plus the incremental strains $\dot{\varepsilon}_{ij}$, $\dot{e}_P$ and $\dot{e}_{P,i}$.

4.3 The non-incremental SGP model

Non-incremental SGP theories were proposed by Gudmundson (2004) and Gurtin and Anand (2005) with essential aspects of their implementation provided by Fleck and Willis (2009a,b). This class of theories employs stress quantities that are not fixed in the current state but depend on the increments of plastic strain and strain gradients. The construction underlying

the non-incremental theories ensures satisfaction of the thermodynamic requirement that plastic dissipation is non-negative. A basic rate-independent non-incremental version will be employed in this paper to illustrate the issues that arise when one attempts to use this class of theories for modeling plastic bifurcation and buckling phenomena. The plastic deformation in the non-incremental model is taken to be entirely dissipative such that in the notation introduced earlier $q_{ij}^{R} = \tau_{ijk}^{R} = 0$, $q_{ij} = q_{ij}^{UR}$ and $\tau_{ijk} = \tau_{ijk}^{UR}$. Following notation and developments similar to those of Fleck and Willis (2009a,b), generalized stress and strain-rate vectors are defined,

$$\mathbf{\Sigma} = \sqrt{3/2}\left(q_{ij}, \ell^{-1}\tau_{ijk}\right) \text{ and } \dot{\mathbf{E}}_P = \sqrt{2/3}\left(\dot{\varepsilon}_{ij}^{P}, \ell\dot{\varepsilon}_{ij,k}^{P}\right), \tag{4.14}$$

with $\left|\mathbf{\Sigma}\right| \equiv \Sigma = \sqrt{(3/2)\left(q_{ij}q_{ij} + \ell^{-2}\tau_{ijk}\tau_{ijk}\right)}$ and $\left|\dot{\mathbf{E}}_P\right| = \dot{E}_P$ as the unrecoverable generalized strain rate defined earlier such that $E_P = \int \dot{E}_p$. The yield condition for this theory is $\Sigma = \sigma_0(E_p)$ where $\sigma_0(\varepsilon_P)$ is the plastic portion of the tensile stress-strain curve defined earlier. With $\Sigma = \sigma_0(E_p)$ regarded as a yield surface in generalized stress space, $\mathbf{\Sigma}$ is an outward normal.

As in the incremental models, the model used here has $\sigma_{ij} = L_{ijkl}^{e}\varepsilon_{kl}^{e} = L_{ijkl}^{e}(\varepsilon_{kl} - \varepsilon_{kl}^{P})$. The other stress components are defined by the constitutive requirement

$$\mathbf{\Sigma} = \sigma_0(E_P)\frac{\dot{\mathbf{E}}_P}{\dot{E}_P}, \quad \text{or } q_{ij} = \frac{2}{3}\sigma_0(E_P)\frac{\dot{\varepsilon}_{ij}^{P}}{\dot{E}_P} \ \& \ \tau_{ijk} = \frac{2}{3}\ell^2\sigma_0(E_P)\frac{\dot{\varepsilon}_{ij,k}^{P}}{\dot{E}_P} \tag{4.15}$$

As in the case of the three incremental models used here, this choice reduces to the input stress-strain curve in uniaxial tension, and it coincides with the classical J_2 flow theory in the absence of plastic strain gradients or with $\ell = 0$. Further, for strictly proportional straining this version of the non-incremental theories coincides with Model B. The plastic work increment in this theory satisfies $\mathbf{\Sigma}\bullet\dot{\mathbf{E}}_P = \sigma_0(E_P)\dot{E}_P \geq 0$ guaranteeing non-negative dissipation.

Non-incremental theories differ significantly from incremental theories in problems where abrupt changes occur in the direction of the strain-rate $\dot{\mathbf{E}}_P$, such as in most plastic buckling problems, because the stress quantities (q_{ij}, τ_{ijk}) defined in (4.15) are not known in the current state but depend on the solution increment itself. Consequences of this construction for physical predictions have been discussed in Hutchinson (2012), and Fleck et al. (2014, 2015). Relevant to the present study of column buckling in the plastic range is the finding in Fleck et al. (2014) that a planar layer undergoes an elastic bending response, according to the non-

incremental theory, when it is deformed uniformly into the plastic range in plane strain compression (or tension) and then subject to an increment of bending. In other words, the incremental bending stiffness/depth D according to this class of theories is the elastic bending stiffness. Except in the range immediately exceeding plastic yield, an elastic incremental bending stiffness implies that bifurcation into a buckling mode will not occur. The consequences of this seemingly unphysical prediction will be explored in Section 6 by including initial imperfections and carrying out detailed buckling computations for the non-incremental theory.

5. The 2D plane strain bifurcation problem for buckling of the clamped column

The exact plane strain analysis carried out in this section follows similar previous analyses by Hill and Hutchinson (1975), Young (1976), Needleman (1979), and Benallal and Tvergaard (1995). The paper by Benallal and Tvergaard is especially relevant because that bifurcation study is also carried out for a SGP material and considerable attention has been paid to some of the underlying mathematical issues that need not be readdressed here. Our starting point will be the quadratic functional governing the bifurcation problem for the uniformly compressed rectangular block of dimension $2h \times 2L$ in the compressed state with the geometry and notation given in Fig.1. In the pre-bifurcation state the rectangular column has been loaded monotonically in uniform plane strain compression into the plastic range with $\sigma_{11} = -2\sigma_0(e_P)/\sqrt{3}$ and $e_P = \varepsilon_P = -2\varepsilon_{11}^P/\sqrt{3}$.

The unknown field quantities in the plane strain bifurcation problem are the increments, $\dot{u}_1(x_1, x_2)$, $\dot{u}_2(x_1, x_2)$ and $\dot{e}_P(x_1, x_2)$, subject to the incompressibility condition $\dot{u}_{1,1} + \dot{u}_{2,2} = 0$. The quadratic bifurcation functional is

$$\begin{aligned}\Phi(\dot{u}_1, \dot{u}_2, \dot{e}_P, \lambda) = (E_{ps}/4)\int_{-h}^{h} dx_2 \int_{-L}^{L} dx_1 \Big\{ & 2\left(\dot{u}_{1,1} + \sqrt{3}\,\dot{e}_P/2\right)^2 + \frac{1}{2}\left(\dot{u}_{1,2} + \dot{u}_{2,1}\right)^2 + \frac{1}{2}a_1 \dot{e}_P{}^2 \\ & + \frac{1}{2}a_2 \ell^2 \left(\dot{e}_{P,1}{}^2 + \dot{e}_{P,2}{}^2\right) + \frac{\sigma_{11}}{E_{ps}}\left((\dot{u}_{2,1}{}^2 - \dot{u}_{1,1}{}^2 - \frac{1}{2}(\dot{u}_{1,2} + \dot{u}_{2,1})^2) \right) + \lambda\left(\dot{u}_{1,1} + \dot{u}_{2,2}\right) \Big\}\end{aligned} \tag{5.1}$$

where $E_{ps} = 4E/3$ is the plane strain elastic tensile modulus (for an elastically incompressible material) and $(\ )_{,i} = \partial(\ )/\partial x_i$. The incompressibility condition is enforced with a Lagrangian

multiplier, λ, and elsewhere in the integrand contributions involving $\dot{u}_{2,2}$ have been replaced by the substitution $\dot{u}_{2,2} = -\dot{u}_{1,1}$. For all three incremental theories,

$$a_1 = \frac{3}{E}\frac{d\sigma_0(e_P)}{de_P} = \frac{3E_t / E_{ps}}{\left(1 - E_t / E_{ps}\right)} \tag{5.2}$$

where E_t is the plane strain tangent modulus at e_P, and a_2 is defined for each of the theories by (2.6). The top and bottom surfaces are traction-free such that there are no constraints on the variations of the displacement increments or $\dot{e}_P$, while on the ends, the shear traction increments vanish and the eigenmode contribution to the bifurcation solution is constrained such that $\dot{u}_1 = 0$.

The details at arriving at (5.1) in the absence of gradient hardening are given in Hill and Hutchinson (1975) and for a problem with strain gradient hardening by Benallal and Tvergaard (1995). In brief, the stress increments in $\varphi = (\dot{\sigma}_{ij}\dot{\varepsilon}^e_{ij} + \dot{q}_{ij}\dot{\varepsilon}^P_{ij} + \dot{\tau}_{ijk}\dot{\varepsilon}^P_{ij,k})/2$ are identified as the Jaumann increments of true stress components. The terms in (5.1) multiplied by σ_{11} / E_{ps} arise from transforming to the Jaumann rate within a rigorous finite strain context with increments measured from the current deformed state. The first four terms in the integrand in (5.1) derive from an exact reduction of φ defined for the models in (4.11)-(4.13). In this formulation, the stress σ_{11} in the current configuration is the true stress, ε_{11} is the log strain, and the tangent modulus E_t is the ratio of their increments.

Before carrying out the 2D analysis, we digress to interject the derivation of the incremental bending stiffness employed in the 1D buckling analysis in Sections 3 and 4.

5.1 The incremental bending stiffness D under increments of uniform stretch and bending

We impose strain increments which are independent of x_1 on the block such that $\dot{\varepsilon}_{11} = -\dot{\varepsilon}_0 - \dot{\kappa}x_2$ and produce solutions governed by (5.1) with increments of strain gradients and plastic strain that are independent of x_1, disregarding the ends of the block. Our objective is to derive the incremental bending stiffness/depth D under conditions of uniform bending and stretching such that plastic loading occurs across the block. The 2D functional (5.1) reduces to a 1D functional of $\dot{e}_p(x_2)$ over the interval $-h \le x_2 \le h$ with $\dot{\varepsilon}_0$ and $\dot{\kappa}$ being prescribed

$$\Phi(\dot{e}_P) = (E_{ps}/4)\int_{-h}^{h}\left\{2\left(\dot{\varepsilon}_0 + \dot{\kappa}x_2 - \sqrt{3}\,\dot{e}_P/2\right)^2 + \frac{1}{2}a_1\dot{e}_P{}^2 + \frac{1}{2}a_2\ell^2\left(\frac{d\dot{e}_P}{dx_2}\right)^2\right\}dx_2 \tag{5.3}$$

The terms in (5.1) multiplying σ_{11} have been neglected anticipating that $|\sigma_{11}| << E_t$. Note, however, that the term $\sigma_{11}\dot{u}_{2,1}{}^2$ in (5.1) is critical to the stability of the column. Through its contribution, $-\int_{-L}^{L} P(dW/dx_1)^2 dx_1$, to the 1D functional governing buckling, it generates the term, Pd^2W/d^2x_1, in the 1D buckling equation (3.1).

The solution to the variational equation generated by (5.3), assuming no constraint on plasticity at the top and bottom surfaces and combinations of $\dot{\varepsilon}$ and $\dot{\kappa}$ such that $\dot{e}_P \geq 0$ across the block, is

$$\dot{e}_P = \frac{2\sqrt{3}}{3+a_1}\left[\dot{\varepsilon}_0 + \dot{\kappa}h\left(\frac{x_2}{h} - \alpha\frac{\sinh(x_2/(\alpha h))}{\cosh(1/\alpha)}\right)\right] \tag{5.4}$$

with $\alpha = \sqrt{a_2/(3+a_1)}\ell/h$ or re-expressed as (2.3). The requirement that $\dot{e}_P$ be non-negative is

$$\dot{\varepsilon}_0 \geq |\dot{\kappa}|h\left(1 - \alpha\tanh(1/\alpha)\right) \tag{5.5}$$

The incremental bending stiffness in (2.2) can be evaluated using either $\frac{1}{2}\left(S\dot{\varepsilon}_0{}^2 + D\dot{\kappa}^2\right) = \Phi(e_P)$ or $D\dot{\kappa} = -\int_{-h}^{h}\dot{\sigma}_{11}x_2 dx_2$, where the latter follows from the principle of virtual work (4.1) using the fact that there are no tractions on the top and bottom surfaces of the block.

5.2 The 2D plane strain buckling solution

The field equations for $(\dot{u}_1, \dot{u}_2, \dot{e}_P)$ rendering Φ in (5.1) stationary admit a uniform solution

$$\dot{u}_1/h = -\dot{\varepsilon}_0 x,\ \dot{u}_2/h = \dot{\varepsilon}_0 y,\ \dot{e}_P = (2/\sqrt{3})(1 - E_t/E_{ps})\dot{\varepsilon}_0 \text{ for } \dot{\varepsilon}_0 \geq 0 \tag{5.6}$$

and separated solutions for the eigenmode problem of the form

$$(\dot{u}_1/h, \dot{u}_2/h, \dot{e}_P, \lambda) = \left(U(y)\sin(\xi x), V(y)\cos(\xi x), \eta(y)\cos(\xi x), Q(y)\cos(\xi x)\right) \tag{5.7}$$

where $(x, y) = (x_1, x_2)/h$, $(\ )' = d(\ )/dy$, $\xi = \pi h/L$. The uniform solution satisfies the boundary conditions and is associated with an increment of σ_{11}. The separated solution satisfies the symmetry about $x = 0$ and zero shear traction increment and $\dot{u}_1 = 0$ on the ends. Because the functional (5.1) involves only the gradients of u_2 a constant can be added to $V(y)\cos(\xi x)$ so as to satisfy $u_2(\pm L/h, 0) = 0$ as well as $\partial u_2(\pm L/h, y)/\partial x_1 = 0$, consistent with the idealized clamped-clamped boundary which otherwise do not constrain u_2 on the ends. When the separated solution is substituted in (5.1) and the integrations with respect to x are performed, one obtains the reduced functional for the eigenvalue problem

$$\frac{\Phi}{E_{ps}hL/4} = \int_{-1}^{1}\Bigg\{\left(2(\xi U + \sqrt{3}\,\eta/2\right)^2 + \frac{1}{2}\left(U' - \xi V\right)^2 + \frac{1}{2}a_1\eta^2 + \frac{1}{2}a_2(\ell/h)^2\left((\xi\eta)^2 + \eta'^2\right)$$
$$+\frac{\sigma_{11}}{E_{ps}}\left((\xi V)^2 - (\xi U)^2 - \frac{1}{2}(U' - \xi V)^2)\right) + Q\left(\xi U + V'\right)\Bigg\}dy$$

(5.8)

The system of ordinary differential equations (odes) and boundary conditions rendering Φ stationary is

$$\left.\begin{aligned} -2A_2U'' + 2\xi^2A_1U + 2\xi A_2V' + \xi A_4\eta - \xi Q = 0 \\ Q' + 2\xi^2A_3V - 2\xi A_2U' = 0 \\ -2A_6\eta'' + \xi A_4U + 2A_5\eta + 2\xi^2A_6\eta = 0 \\ V' + \xi U = 0 \end{aligned}\right\}, \quad -1 \le y \le 1 \tag{5.9}$$

and

$$U' - \xi V = 0,\ Q = 0,\ \eta' = 0, \text{ on } y = \pm 1 \tag{5.10}$$

with $A_1 = 2 - 2\sigma_{11}/E_{ps}$, $A_2 = 1/2 - \sigma_{11}/E_{ps}$, $A_3 = 1/2 + \sigma_{11}/E_{ps}$, $A_4 = 2\sqrt{3}$, $A_5 = (3 + a_1)/2$, and $A_6 = a_2(\ell/h)^2/2$. Anti-symmetry allows one to restrict attention to the interval $0 \le y \le 1$ with $U = Q = \eta = 0$ on $y = 0$. The system of odes is 6th order with constant coefficients. The eigenvalue is the critical value of the compressive strain ε_0, or, equivalently, the associated value of e_P, which enters all the coefficients but A_4. We have pursued two solution methods. One follows the procedures of Hill and Hutchinson (1975) and, more specifically, that of

Benallal and Tvergaard (1995) by generating the linearly independent solutions to (5.9) and then expressing the boundary conditions (5.10) in terms of the amplitudes of the independent solutions. Solving the resulting algebraic system for the critical eigenvalue and eigenmode requires numerical computation. A more straightforward method requiring less analytical effort involves reducing (5.9) to 6 first order odes and using a standard ode solver to generate the solutions and boundary conditions. To implement this second scheme for the eigenvalue problem, we imposed all of the boundary conditions except $Q=0$ on $y=1$, replacing it by $V=1$ on $y=1$, varying ε_0 (or, e_P) until $Q=0$ on $y=1$ is satisfied.

The example shown in Fig. 5 illustrates the results of these procedures for Model C and it also gives a clear indication of the extensive range of accuracy of the 1D buckling analysis presented in Section 3. There is almost no error in the 1D result for L/h as small as 10, and the error for rather stubby columns with $L/h=5$ is still quite small. A gratifying outcome of the exact plane strain analysis is that the much simpler 1D approach should be adequate for all but extremely stubby columns. Analogous conclusions are likely to apply a broader range of problems in the plastic buckling of plates and shells.

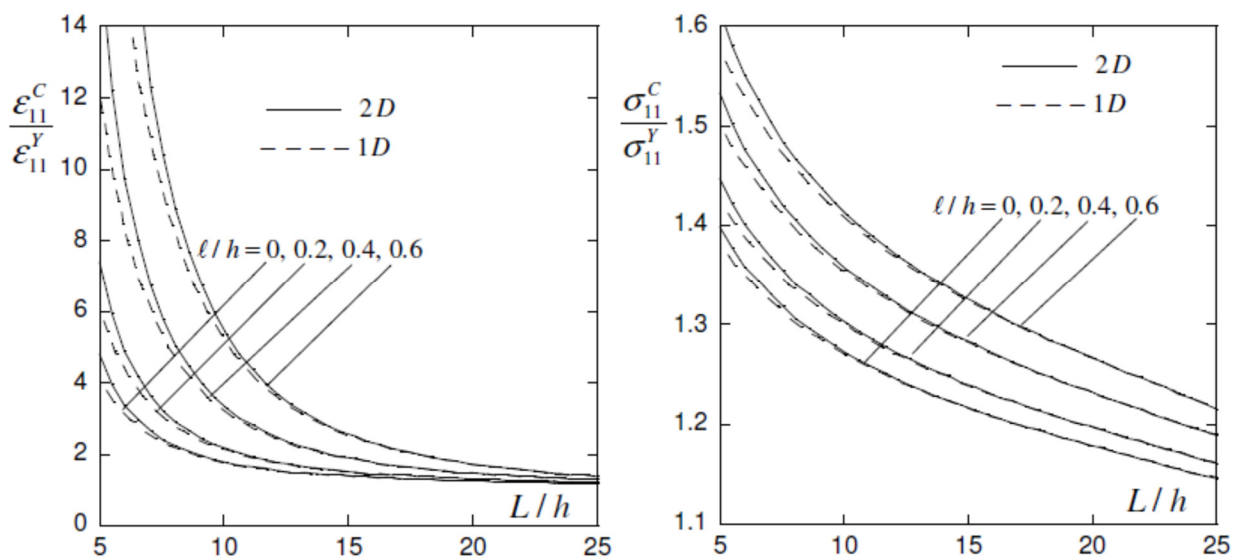

Fig 5 Comparison of exact 2D plane strain buckling analysis and 1D buckling analysis for Model C. The results apply to a wide column of thickness $2h$ and length $2L$ which is clamped at both ends and subject to plane strain compression. The compressive strain ε_{11}^C and stress σ_{11}^C at the onset of buckling are normalized by ε_{11}^Y and σ_{11}^Y, respectively. Curves are presented for three

values of the dimensionless gradient length parameter ℓ / h plus conventional plasticity with $\ell / h = 0$, and with $\varepsilon_{11}^{Y} = -\sqrt{3}\sigma_Y / 2E$, $\sigma_{11}^{Y} = -2\sigma_Y / \sqrt{3}$, $\sigma_Y / E = 0.003$, $N = 0.2$ and $k = 1$.

6. Finite element modeling of 2D plane strain buckling at small scales: non-incremental plasticity

The finite element analysis builds upon the finite strain framework developed in Nielsen and Niordson (2019) for the version of non-incremental SGP theory by Fleck and Willis (2009a,b). This section aims to further explore the behavior of micron size wide columns that buckle in the plastic range specifically for a non-incremental SGP theory which, as noted earlier in the paper, does not predict bifurcation buckling when the column is perfectly straight. In this section, we study the behavior when slight initial imperfections from straightness are introduced. The modeling framework adopts a rate-dependent (visco-plastic) version of the SGP theory presented in Section 4.3, such that

$$q_{ij} = \frac{2}{3}\sigma_0(E^P)\left(\frac{\dot{E}^p}{\dot{\varepsilon}_R}\right)^m \frac{\dot{\varepsilon}_{ij}^p}{\dot{E}^p} \quad \text{and} \quad \tau_{ijk} = \frac{2}{3}\ell^2\sigma_0(E^P)\left(\frac{\dot{E}^p}{\dot{\varepsilon}_R}\right)^m \frac{\dot{\varepsilon}_{ij,k}^p}{\dot{E}^p}, \tag{6.1}$$

and the visco-plastic potential is

$$\Phi\left[E^p.\dot{E}^p\right] = \sigma_0(E^P)\frac{\dot{\varepsilon}_R}{m+1}\left(\frac{\dot{E}^p}{\dot{\varepsilon}_R}\right)^{m+1}, \tag{6.2}$$

with m being the rate sensitivity exponent and $\dot{\varepsilon}_R$ the reference strain rate. The expressions for the micro- and higher-order stresses are identical to (4.15), apart from the rate-dependent factor $\left(\dot{E}^p/\dot{\varepsilon}_R\right)^m$ (also discussed in Fleck et al., 2015). As remarked in Section 4.3, the rate-independent limit of this version of non-incremental constitutive theory coincides with Model B for proportional straining. In the simulations to follow, the rate-independent limit is approached by considering low rate-sensitivity ($m = 0.01$) and strain rates corresponding the reference strain rate ($\dot{\varepsilon}_R L/\dot{\Delta} = 1$).

The finite strain model is based on an updated Lagrangian formulation, using the Jaumann rate, $\overset{\nabla}{\tau}_{ij} = \dot{\tau}_{ij} - \dot{\omega}_{ik}\tau_{kj} - \tau_{ik}\dot{\omega}_{jk}$, such that the elastic relation is; $\overset{\nabla}{\tau}_{ij} = L_{ijkl}^e(\dot{\varepsilon}_{kl} - \dot{\varepsilon}_{kl}^p)$. Here, $\dot{\omega}_{ij} = (\dot{u}_{i,j} - \dot{u}_{j,i})/2$ is the spin rate. The displacements, u_i, are the vector sum; $\boldsymbol{u} = \boldsymbol{X} - \boldsymbol{x}$, where $\boldsymbol{X}$ is the position of the material in the current configuration, and $\boldsymbol{x}$ is its position in the reference configuration. The virtual work principle is stated in (4.1) for the current configuration,

and the finite element implementation makes use of Minimum Principle I and II first outlined by Fleck and Willis (2009b). In the current configuration, stationarity of Minimum Principle I yields

$$\int_V q_{ij}\delta\dot{\varepsilon}_{ij}^p + \tau_{ij,k}\delta\dot{\varepsilon}_{ij,k}^p \,\mathrm{d}V = \int_V s_{ij}\delta\dot{\varepsilon}_{ij}^p \,\mathrm{d}V + \int_S t_{ij}\delta\dot{\varepsilon}_{ij}^p \,\mathrm{dS}, \tag{6.3}$$

and stationarity of Minimum Principle II gives

$$\int_V \sigma_{ij}\delta\dot{\varepsilon}_{ij} \,\mathrm{d}V = \int_S T_i\delta\dot{u}_i \,\mathrm{dS}. \tag{6.4}$$

when only accounting for the dissipative part of the micro- and higher-order stresses. Equation (6.4) is rewritten using the original reference configuration following McMeeking and Rice (1976), Niordson and Redanz (2004), such that the incremental form becomes

$$\int_{V_0} \tau_{ij}^*\delta\dot{\varepsilon}_{ij} - \sigma_{ij}(2\dot{\varepsilon}_{ik}\delta\dot{\varepsilon}_{kj} - u_{k,j}\delta\dot{u}_{k,i}) \,\mathrm{d}V = \int_{S_0} \dot{T}_i^0\delta\dot{u}_i \,\mathrm{dS}. \tag{6.5}$$

By discretizing (6.3) and (6.5) using the finite element method, a staggered solution approach for determining the plastic strain rate field, $\dot{\varepsilon}_{ij}^p$, and the displacement increments, $\dot{u}_i$, is adopted. In Step 1, the stress field in the current configuration is assumed and this allows iteration on a solution to (6.3) that delivers the plastic strain rate field. In Step 2, the displacement increments are determined from (6.5) based on the plastic strain rate field from Step 1. The reader is referred to Niordson and Nielsen (2019) for further details on the numerical procedure. A standard finite element interpolation is used such that bi-linear elements discretize (6.3) and bi-quadratic elements discretize (6.4), using 2-by-2 Gauss integration in both element types (see also Nielsen and Niordson, 2013).

Figure 1 illustrates the boundary value problem with the imposed conditions: zero surface tractions on the sides and $\dot{u}_1 = \pm\dot{\Delta}$, $T_2 = 0$, and $t_{ij} = 0$ at $x_1 = \pm L$. The undeformed column is discretized by elements of size $L_e \times L_e = (h/6) \times (h/6)$, such that 12 elements are used through-thickness of the column (in the x_2-direction, see Fig. 1). A mesh-convergence check has been performed. Introducing an initial imperfection, with the eigenmode shape in Eq. (3.2) and amplitude δ (the initial lateral deflection at the center of the column). As noted in Section 4.3, the adopted non-incremental (Fleck and Willis, 2009b) class of theories yields an incremental bending stiffness equal to the elastic stiffness when the column is perfectly straight, implying that bifurcation into buckling will not occur in the plastic range. Thus, the purpose of the study in

this section is to investigate whether realistic plastic buckling behavior ensues when imperfections are introduced.

Figure 6 shows the load-displacement response, in terms of normalized average end-stress and average overall strain, for two columns with very different gradient strengthening. The conventional limit, represented to a good approximation here with a very small material length parameter, $\ell/h = 0.01$, shows a reasonable match to the results from the 1D plastic bifurcation analysis for both the critical strain (see Fig. 3, Model B) and the critical stress (see Fig. 4, Model B). Moreover, the load-carrying capacity of the column drops dramatically after attaining its maximum in the plastic post-buckling response, as expected from earlier studies (Hutchinson, 1974). Imperfection size plays a role in the response in the conventional limit, but the effect is seen to be rather limited when the imperfections are relatively small, contrasting with the column response when the gradient length parameter is large. The plot on the right in Fig. 6 shows the column response for the case $\ell/h = 0.6$. In line with Figs. 3 and 4, the gradient enhanced material stabilizes the column such that the critical stress and strain at buckling increase for increasing ℓ/h. However, the results predicted on the right in Fig. 6 are almost certainly unrealistic large from a physical standpoint. Note, for example, that the strain at bifurcation predicted in Fig. 3 for the incremental version of Model B is $\varepsilon_{11} / \varepsilon_{11}^{Y} \cong 3$ and this is roughly one half the strain at buckling for the largest imperfection considered in Fig. 6. Moreover, the trend in Fig. 6 for $\ell/h = 0.6$ suggests that the strain at buckling continues to increase as the imperfection amplitude decreases, consistent with the fact that no bifurcation is possible for the non-incremental theory when the column is perfect.

In fact, according to the non-incremental theory, more stubby columns undergo such extreme end-shortening that the thickening of the column becomes important, preventing the column from buckling. Figure 7 displays the seemingly unbounded increase of the critical strain with diminishing imperfection size for two length to thickness ratios and four values of the gradient length parameter. For both length to thickness ratios, the result for the conventional limit ($\ell/h = 0.01$) displays relatively little effect of the imperfection size in the range considered as one would expect, however the critical buckling strain is expected to drop for larger imperfections (not shown here). In comparison, the critical buckling strain shows no sign of leveling off for diminishing imperfection size when the gradient length parameter is not small.

The reluctance to buckle at a small scale according to the non-incremental theory is even more pronounced for more stubby columns ($L/h = 10$) considered on the right in Fig. 7.

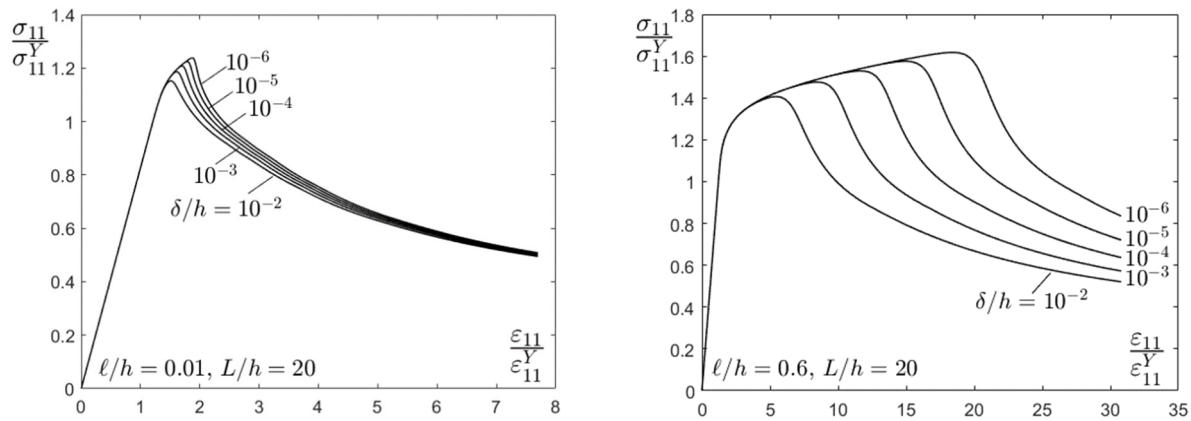

Fig 6 Normalized average compressive stress versus normalized average compressive strain for two values of the gradient length parameter; a very small value, $\ell/h = 0.01$, and a relatively large value, $\ell/h = 0.6$, and for several imperfection sizes; $\delta/h = 10^{-6}$, 10^{-5}, 10^{-4}, 10^{-3}, and 10^{-2}. The column height is $L/h = 20$. In these plots $\varepsilon_{11}^Y = -\sqrt{3}\sigma_Y/2E$, $\sigma_{11}^Y = -2\sigma_Y/\sqrt{3}$, $\sigma_Y/E = 0.003$, $N = 0.2$, and $k = 1$. Note that for the column on the right with $\ell/h = 0.6$, the bifurcation strain for the incremental version with Model B from Fig. 3 is $\varepsilon_{11}/\varepsilon_{11}^Y \cong 3$.

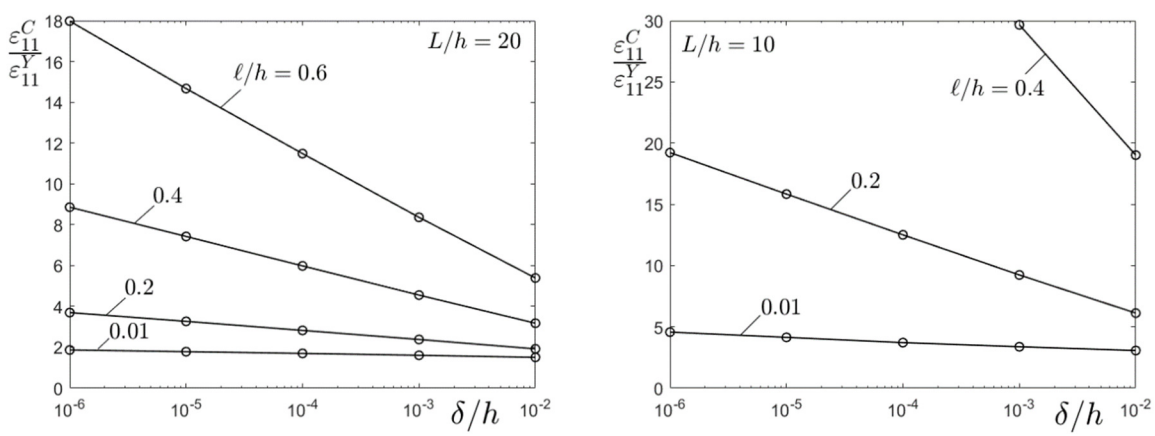

Fig 7 Normalized critical buckling strain versus the imperfection size, δ/h, for four values of the gradient length parameter $\ell/h = 0.01$, 0.2, 0.4 and 0.6, and two different column length to thickness ratios $L/h = 20$ (left figure) and $L/h = 10$ (right figure). In these plots $\varepsilon_{11}^Y = -\sqrt{3}\sigma_Y/2E$, $\sigma_{11}^Y = -2\sigma_Y/\sqrt{3}$, $\sigma_Y/E = 0.003$, $N = 0.2$, and $k = 1$.

7. Conclusions

The three incremental strain gradient plasticity models considered in this paper predict that buckling resistance in the plastic range is substantially enhanced if the ratio of the material length parameter to the column thickness, ℓ / h, is greater than about 0.2 or 0.4. Experimental measurements of ℓ yield values typically in the range of a fraction of a micron to perhaps 5 microns, with softer metals tending to have a larger length parameter than those that are harder. Of course, to some extent, the measured value depends on the constitutive model employed to analyze the test and back out the length. Given the range, $0.1\mu m < \ell < 5\mu m$, the present predictions suggest that columns with thicknesses in the range, $0.5\mu m < h < 25\mu m$, depending on the material, will display enhanced plastic buckling resistance due to strain gradients. This study shows that there is considerable sensitivity of the predictions to the details of the SGP models. In Section 4.2, we have argued Model C appears to have the most favorable attributes of the three incremental models considered here.

While non-incremental formulations have some attractive features for numerical implementation, the present study suggests that they have severe limitations for analyzing column buckling in the plastic range. It has been shown that not only does this class of theories predict that bifurcation into a buckling mode is effectively excluded, but even when imperfections are introduced, these theories predict that plastic buckling will be postponed to unrealistically large strains and stresses. There is good reason to believe that the inadequacy of the non-incremental SGP theories for column buckling will carry over to other instabilities in the plastic range, such as the plastic buckling of plates and shells and to more exotic phenomena such as shear bands and surface wrinkles.

The more complicated and accurate 2D plane strain bifurcation analysis has shown that the 1D analysis based on Euler-Bernoulli beam theory with input of the gradient enhanced bending stiffness retains good accuracy for all but very stubby columns, assuming an incremental constitutive model is employed. For the incremental models, it remains to explore the initial post-buckling behavior and the effect of initial imperfections. It also remains to determine the gradient enhancement of the incremental bending stiffness for columns of various cross-sections.

Acknowledgements

KLN is financially supported by VILLUM FOUNDATION EXPERIMENT in the project ``Micron-Scale Crashworthiness", grant no. 00028205.

References

Benallal, A., Tvergaard, V., 1995. Nonlocal continuum effects on bifurcation in the plane strain tension-compression test. J. Mech. Phys. Solids 43, 741-770.

Engesser, F., 1889. Ueber die knickfestigkeit geradu strabe. Z. Architek. Ing. 38, 455.

Fleck, N.A., Willis, J.R., 2009a. A mathematical basis for strain-gradient plasticity theory. Part I: Scalar plastic multiplier. J. Mech. Phys. Solids 57, 161–177.

Fleck, N.A., Willis, J.R., 2009b. A mathematical basis for strain-gradient plasticity theory. Part II: Tensorial plastic multiplier. J. Mech. Phys. Solids 57, 1045–1057.

Fleck, N.A., Hutchinson, J.W., Willis, J.R., 2014. Strain gradient plasticity under non-proportional loading. Proc. R. Soc., A. 470, 20140267.

Fleck, N.A., Hutchinson, J.W., Willis, J.R., 2015, Guideline for constructing strain gradient plasticity theories. J. Appl. Mech. 82, 071002, 1-10.

Gudmundson, P. A., 2004. A unified treatment of stress gradient plasticity. J. Mech. Phys. Solids, 52, 1378-1406.

Gurtin, M. E., Anand, L., 2006. A theory of strain-gradient plasticity for isotropic, plastically irrotational materials-Part I: Small deformations. J. Mech. Phys. Solids, 53, 1624-1649.

Hill, R., 1958. A general theory of uniqueness and stability in elastic-plastic solids. J. Mech. Phys. Solids 6, 236-249.

Hill, R., Hutchinson, J. W., 1975. Bifurcation phenomena in the plane strain tension test. J. Mech. Phys. Solids 23, 239-264.

Hutchinson, J.W., 1974. Plastic Buckling. Adv. Appl. Mech. 14, 67–144.

Hutchinson, J.W., 2012. Generalizing J2-flow theory: Fundamental issues in strain gradient plasticity. Acta Mech. Sin., 28, 1078-1086.

Kyriakides, S., Corona, E., 2007. Mechanics of Off-Shore Pipelines: Vol. 1. Buckling and Collapse. Elsevier, Oxford, UK.

Kyriakides, S., Lee, L-H., 2020. Mechanics of Off-Shore Pipelines: Vol. 2. Buckle Propagation and Arrest. Elsevier, Oxford, UK.

McMeeking, R.M., Rice, J.R., 1975. Finite-element formulations for problems of large elastic-plastic deformation. Int. J. Solids Struct. 11, 601-616.

Muhlhaus, H. B., Aifantis, E. C., 1991. A variational principle for gradient plasticity. Int. J. Solids Struct., 28, 845-857.

Needleman, A., 1979. Non-normality and bifurcation in plane strain tension-compression. J. Mech. Phys. Solids 27, 231-254.

Nellemann, C., Niordson, C.F., Nielson, K.L., 2017a. An incremental flow theory for single crystal plasticity incorporating train gradients. Int. J. Solids Struct. 110-111, 230-250.

Nellemann, C., Niordson, C.F., Nielson, K.L., 2017b. Hardening and strengthening behavior in rate-independent strain gradient crystal plasticity. Eur. J. Mech. A/Solids 67, 157–168.

Nielsen, K.L., Niordson, C.F., 2013. A 2D finite element implementation of the Fleck-Willis strain-gradient flow theory. Eur..J. Mech. A/Solids 41, 134–142.

Nielsen, K.L., Niordson, C.F., 2019. A finite strain FE-Implementation of the Fleck-Willis gradient theory: Rate Independent versus visco-plastic formulation. European journal of Mechanics A/Solids 75, 389–398.

Niordson, C.F., Redanz, P., 2004. Size-effects in plane strain sheet-necking. J. Mech. Physics Solids 11, 2431-2454.

Sewell, M.J., 1963. A general theory of elastic and inelastic plate failure. Part I. J. Mech Phys. Solids 11, 377-393.

Shanley, F.R., 1947. Inelastic column theory. J. Aeronaut. Sci. 14, 261-267.

von Karman, Th, 1910, Untensuchungen über knickfestigkeit, mitteilungen über forschungsarbeiten. VDI (Ver. Deut. Ing.), Forschungsh. 81.

Young, N.J.B., 1976. Bifurcation phenomena in the plane strain compression test. J. Mech. Phys. Solids 24, 77-91.